# OPPOSING SOUTHERN OCEAN CLIMATE PATTERNS AS REVEALED BY TRENDS IN REGIONAL SEA ICE COVERAGE

S. E. STAMMERJOHN and R. C. SMITH
*Institute for Computational Earth System Science, University of California, Santa Barbara, CA 93106, U.S.A.*

**Abstract.** The 16.8 year sea ice record (November 1978 to August 1995) derived from satellite passive microwave data shows evidence of contrasting climate patterns in the Southern Ocean as indicated by persistent opposing trends in regional sea ice coverage. Southern Ocean regions adjoining the south Atlantic, south Indian and southwest Pacific Oceans show *increasing* trends in sea ice coverage, particularly during non-winter months, while regions adjoining the southeast Pacific Ocean show *decreasing* trends in sea ice coverage, particularly during summer months. The data are compiled from three successive passive microwave sensors from which two separate time-series are analyzed. The first includes the data originally released by the National Snow and Ice Data Center (NSIDC) which have not been significantly adjusted to account for differences in the successive sensors, while the second includes data recently released by NSIDC which have been rigorously adjusted (Cavalieri et al., 1997) to account for differences between sensors. Although the significance of many of the increasing trends detected in the original time-series decrease in the reanalyzed time-series, the overall pattern of contrasting trends remains evident. These trends have important implications for the southern hemisphere heat budget and surface albedo as well as for marine ecosystems associated with various sea ice habitats. Other evidence of contrasting climate patterns with respect to southern hemisphere atmospheric circulation is explored. Due to the relatively short sea ice record, it still remains to be seen whether these trends are natural decadal variation or indicative of global climate change. However, the persistent opposition in Southern Ocean regional ice coverage is noteworthy and may well be studied using global circulation models in order to better define potential positive and negative feedbacks for global change scenarios.

## 1. Introduction

Sea ice plays an important role in the global climate system by influencing the regional heat budget, surface albedo, and consequently oceanic and atmospheric circulation. Several studies have suggested that long-term variations in sea ice coverage may be indicative of possible large-scale and long-term climatic change (Fletcher, 1969; Sissala et al., 1972; Budd, 1975; Kukla and Garvin, 1981; Fletcher et al., 1982; Zwally et al., 1983a; Zwally et al., 1983b; Parkinson et al., 1987; Carleton, 1989; Jacka, 1990). Other studies have detected quasi-periodic El Niño/Southern Oscillation (ENSO) signals in both polar sea ice covers suggesting linkages between interhemispheric climate trends and sea ice (Gloersen, 1995; White and Peterson, 1996; Smith et al., 1996). The strong seasonality and interannual variability of sea ice also impacts the polar marine ecosystem, from primary production to the survival rates and distributions of prey and predators (Hunt, 1991; Ross and Quetin, 1991; Fraser et al., 1992; Ainley et al., 1994; Smith et al., 1995; Siegel and Loeb, 1995).

*Climatic Change* **37:** 617–639, 1997.

To date, attempts to find possible trends in polar sea ice coverage using various satellite data have made differing conclusions depending on the time period and sea ice parameter studied. For example, early analyses of Antarctic sea ice extent, using mainly visible and infrared satellite data, indicate an increase in sea ice extent from 1966 to 1973 (Sissala et al., 1972; Streten, 1973; Zwally et al., 1983a). Using Navy–NOAA (National Oceanic and Atmospheric Administration) weekly ice maps, a decrease in Antarctic sea ice extent during the mid 1970's was observed (Kukla and Garvin, 1981), which was then followed by an observed increase from the late 1970's to the early 1980's (Zwally et al., 1983a). Using a longer time-series of the Navy–NOAA weekly ice maps, an overall decrease in Antarctic sea ice extent was observed from 1973 to 1988 (Jacka, 1990). Other studies analyzing the 1978 to 1987 time-series of Antarctic sea ice concentrations derived from multi-frequency passive microwave satellite data have found no significant increasing or decreasing trends in Antarctic sea ice extent, actual sea ice amount or open water area (Gloersen and Campbell, 1991; Gloersen et al., 1992; Parkinson, 1992). More recently, an analysis of a longer time-series of the multi-frequency passive microwave data (1978–1995) again showed no detectable trends in total Antarctic sea ice coverage (Bjørgo et al., 1997). Because of the different types of data and variables analyzed in the above studies, it is difficult to determine whether in the combined observations from 1966 to 1995, there is any long-term decreasing or increasing trend superimposed on the apparent decadal variability.

Presently, the longest, most consistent and continuous sea ice record available is provided by the multi-frequency passive microwave satellite data which began in 1978. This study will analyze the 16.8 year sea ice record provided by that data on several temporal and spatial scales in order to determine whether any trends or patterns in regional Southern Ocean sea ice coverage are detectable. The first multi-frequency passive microwave satellite sensor was the NASA Nimbus 7 Scanning Multichannel Microwave Radiometer (SMMR, October 25, 1978 to August 20, 1987) which was followed by the Defense Meteorological Satellite Program Special Sensor Microwave/Imagers (SSM/I F8 from July 9, 1987 to December 18, 1991, and the SSM/I F11 from December 3, 1991 to September 30, 1995). Our initial analysis of trend patterns was first performed on data originally released by the National Snow and Ice Data Center (NSIDC, 1994; NSIDC, 1996) in which only modest adjustments had been made between the SMMR and SSM/I data. According to Gloersen et al. (1992), the overlap period between the SMMR and SSM/I F8 sensor was used to fine-tune the sea icea algorithm tie-points for both instruments, resulting in a mean difference of $(0.2 \pm 2.5)\%$ for total Antarctic sea ice concentration for the period August 1–20, 1987. However, more recently NSIDC released a reanalysis of the passive microwave sea ice concentrations (NSIDC, 1997), hereafter referred to as the GSFC (Goddard Space Flight Center) reanalysis (Cavalieri et al., 1997), which addresses important problems associated with deriving sea ice concentrations from brightness temperatures measured by sensors with different frequencies, footprint sizes, visit times and calibrations. Using the

same polar mapping grid as in the original data (NSIDC, 1996), the GSFC reanalysis includes: (i) the application of a new landmask (Martino et al., 1995), (ii) the correction of additional instrument drift detected in the SMMR series, (iii) the replacement of bad data, (iv) the adjustment for land-ocean spillover, and (v) intersensor corrections by significantly adjusting the SSM/I sea ice algorithm tie-points to reduce the remaining sea ice extent and area differences during the periods of overlap. Because different land-masks were used in the original SMMR and SSM/I image data, our analysis of these data used a combined SMMR/SSMI landmask in order to remove this bias over the original 16.8 year record.

The intersensor correction made in the GSFC reanalysis appears to make the largest impact and accounts for the greatest differences between the trends observed in the original and the GSFC reanalyzed time-series. This correction is based on adjusting the SSM/I F8 sea ice algorithm tie-points based on linear relationships observed between the brightness temperatures measured by the SMMR and the SSM/I F8 sensors during the overlap period, which unfortunately included only 22 days of common coverage between July 9 and August 20, 1987. In addition, the SSM/I F8 sea ice algorithm tie-point for open water was further tuned to help minimize the differences between the estimates of sea ice extent and area during the overlap period. The SSM/I F11 data were similarly adjusted to the now adjusted SSM/I F8 data during an even shorter overlap period of 16 days (December 3 to 18, 1991) which also coincided with a different season. Although the other corrections clearly make improvements to the overall consistency of the time-series, the intersensor correction is problematic since it results in significantly adjusting the 8 year SSM/I time-series based on very short overlap periods (2–3 weeks) which include seasonal biases as well. Consequently, we feel that it is instructive to present results from both the original and the GSFC reanalyzed time-series, in order to illustrate the differences and to generate awareness of the caveats involved in attempting to achieve long-term consistency in the passive microwave derived sea ice record.

Both the original and GSFC reanalyzed time-series of sea ice concentrations were derived by the NASA Team algorithm (Cavalieri et al., 1984; Gloersen and Cavalieri, 1986; Cavalieri et al., 1995). For further comparison, sea ice concentrations derived by the Goddard Space Flight Center Bootstrap algorithm (Comiso, 1983; Comiso et al., 1984; Comiso, 1995), hereafter referred to as the GSFC Bootstrap algorithm, were determined for the SSM/I period from July 1987 to August 1995 using updated hemispheric tie-points (Comiso, 1995). Unfortunately, GSFC Bootstrap derived sea ice concentrations for the SMMR period were not available at the time of this study, so that only 8.2 years were available for comparisons of the two algorithms.

The sea ice concentration data were spatially and temporally averaged into regional monthly estimates of (i) sea ice extent, the area enclosed by greater than 15% ice concentration (and thus includes areas of open water at sub-pixel resolution), (ii) sea ice area, the actual area covered by sea ice with 15% and greater

ice concentration, and (iii) open water area, the amount of open water inside the boundary of sea ice extent (i.e., sea ice extent minus sea ice area). Since the data do not begin until October 25, 1978, we begin the time-series with November 1978 and end with August 1995, since originally we had access to data only up until that time. Because there were no data from December 3 to January 12, 1988, the monthly average for December 1987 was interpolated between November 1987 and January 1988, noting too that the monthly mean for January 1988 is based on data from January 13 to 31.

The error associated with estimates of sea ice extent depends mostly on the accuracy of the algorithm in distinguishing open ocean from sea ice and has been estimated to be less than 2% for total Southern Ocean sea ice extent (Comiso et al., 1992). The error associated with estimates of sea ice area depends on the accuracy of the algorithm in determining sea ice concentrations between 15 and 100% and is higher than the error associated with sea ice extent estimates. There have been too few validation studies in the Southern Ocean to determine the magnitude of error associated with the estimates of sea ice area and open water area by either the NASA Team or GSFC Bootstrap algorithms. We do know that both the NASA Team and GSFC Bootstrap algorithms typically underestimate sea ice area when compared to other higher resolution satellite derived sea ice concentrations (Comiso et al., 1997).

In order to obtain some sense of validation, annual and seasonal comparisons of sea ice extent, sea ice area and open water area derived from both the NASA Team and GSFC Bootstrap algorithms were made for the period of overlap (7/87–8/95). In agreement with several other studies (Emery et al., 1994; Stammerjohn and Smith, 1996; Comiso et al., 1997), these comparisons show that both algorithms derive similar seasonal and interannual *patterns* in spatially and temporally averaged regional sea ice extent and area. Although the GSFC Bootstrap algorithm with revised tie-points (Comiso, 1995) shows for some regions higher ice concentrations, particularly during winter and spring months, and lower sea ice concentrations, particularly during summer months, correlations of spatially and temporally averaged estimates of sea ice extent, sea ice area and open water area derived by both algorithms are in general very high ($>0.95$), with a few notable exceptions of low correlations in regional open water areas. In this study both algorithms depend on hemispheric tie-points which are empirically derived and which do not account for spatial and temporal variability. Emery et al. (1994) show that sea ice concentration estimates by both algorithms can be greatly improved as well as be made to agree more closely by allowing an adjustment in the sea ice algorithm tie-points. This implies that the differences between the two algorithms can in large part be attributed to the selection of tie-points rather than to differences in the way the two algorithms interpret the surface. Because the estimates of sea ice extent and area by the NASA Team and GSFC Bootstrap algorithms are highly correlated over the period of overlap, we also infer that the repeatability or precision of the sea ice extent and area estimates is high. Since this study is

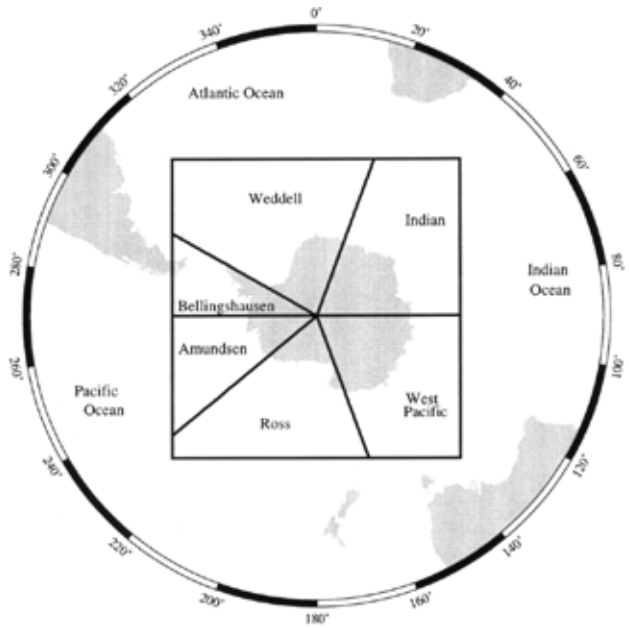


*Figure 1*. Southern Ocean map in polar stereographic projection. The pie sections delineate the six main regions highlighted in this study. The large square outlines the area for which there is sea ice concentration data.

concerned with the detection of trends or patterns, the error associated with actual area amounts is relatively less important as long as that bias is consistent over time. However, there are a few instances when the correlations of regional open water area are low and the bias is not consistent over time, so analyses of those data should be treated cautiously until further validation. Finally, all trends and patterns observed in the 16.8 year time-series derived by the NASA Team algorithm need to be confirmed by comparison with a complete time-series derived by the GSFC Bootstrap algorithm when those data become available.

## 2. Annual and Seasonal Time-Series

Sea ice coverage in the Southern Ocean is marked by high seasonal and regional variability, although total Southern Ocean sea ice extent varies less due to the circumpolar distribution of opposing sea ice anomalies (Zwally et al., 1983b; Parkinson, 1992; Gloersen et al., 1992; Parkinson, 1994). In order to characterize the high seasonal and regional variability, annual and seasonal time-series for both total and regional Southern Ocean sea ice extent, sea ice area and open water area were calculated by *integrating* monthly means for each year or season. The regions of the Southern Ocean used here are as defined in Gloersen et al. (1992) except that the Amundsen (90–130° W) and Bellingshausen (60–90° W) are treated as separate

regions (Figure 1). Before performing linear regression analysis, all annual and seasonal time-series were tested for the presence of serial correlation using the Durbin–Watson $D$-test (Durbin and Watson, 1971). If serial correlation is present, often the error terms in a linear regression analysis will be correlated as well, which would be a violation of one of the fundamental assumptions in linear regression analysis. However, no serial correlation was detected in the annual and seasonal time-series, therefore the number of degrees of freedom in the regression statistics did not have to be penalized accordingly.

Results from the linear regression analyses are shown in Tables I and II. Table I, which includes the sign of the regression slope or trend and the $F$-test confidence level for each region and each variable, shows in general the regional distribution of increasing/decreasing trends for the annual and seasonal time-series. Results from both the original (subscript 1) and the GSFC reanalyzed (subscript 2) time-series are reported. An $F$-test of 90% confidence or more indicates that there is a 10% or less probability of getting a trend of the same magnitude if the time-series were shuffled randomly. Those regressions with an $F$-test of 90% or greater were considered to have detectable trends. For those regressions which met one of two criteria, the magnitude of the slope and standard error are reported in Table II, as well as the correlation coefficient with the GSFC Bootstrap derived sea ice coverage for the period of overlap. The two criteria used in creating Table II were: (i) an $F$-test of 90% or greater in the original time-series and at least 80% or greater in the GSFC reanalyzed time-series, or (ii) an $F$-test of 90% or greater in the GSFC reanalyzed time-series regardless of the $F$-test level in the original time-series. Finally, all figures show for comparison the original and GSFC reanalyzed time-series (as derived by the NASA Team algorithm) as well as the short time-series (7/87–8/95) derived by the GSFC Bootstrap algorithm.

The analysis of the 16 year (1979–1994) *original* time-series of *annual* sea ice coverage revealed a detectable increasing trend in total Southern Ocean sea ice extent and an even stronger increasing trend in sea ice area, resulting in a strong decreasing trend in annual open water area (Table I and Figure 2). Regionally, the only annual time-series which show detectable trends in sea ice extent and/or area are the West Pacific Ocean (increasing ice area) and Ross Sea (increasing sea ice extent and area), while all regions, with the exception of the Ross and Bellingshausen regions, show detectable decreasing trends in annual open water area. In contrast, out of the ten detectable trends observed in the original annual time-series, only two remain detectable in the GSFC reanalyzed time-series, while one remains just below the designated detection level ($F$-test less than 90% but greater than 80%) and one, which was not detectable in the original time-series, is detectable in the GSFC reanalyzed time-series. As shown in Figure 2, the result of adjusting the SSM/I sea ice algorithm tie-points in the GSFC reanalysis has, in effect, shifted the latter portion of the time-series (from 1987 onward) down, in the case of sea ice extent and area, and up, in the case of open water area, which decreases the trends observed in the original time-series.

Table I

Increasing/decreasing trends in total and regional Southern Ocean sea ice extent, sea ice area and open water area. Under Ice Index, the subscripts 1 and 2 refer to the original and GSFC reanalyzed time-series, respectively, and OW stands for open water. $F$-test confidence levels (%) are given in parentheses

| Region | Ice index | Annual (79–94) | Summer (79–95) | Autumn (79–95) | Winter (79–94) | Spring (79–94) |
|---|---|---|---|---|---|---|
| Southern Ocean | $Extent_1$ | +(98.0) | +(97.9) | +(75.2) | +(86.2) | +(84.7) |
| | $Extent_2$ | +(47.1) | +(81.1) | +(56.3) | +(7.9) | +(7.1) |
| | $Area_1$ | +(100.0) | +(99.4) | +(98.7) | +(99.9) | +(99.1) |
| | $Area_2$ | +(66.0) | +(82.9) | +(82.1) | +(6.9) | +(8.1) |
| | $OW_1$ | –(100.0) | +(16.7) | –(100.0) | –(100.0) | –(95.8) |
| | $OW_2$ | –(64.0) | +(46.1) | –(99.6) | +(1.4) | +(0.9) |
| Weddell Sea | $Extent_1$ | +(50.1) | +(95.7) | +(72.8) | +(24.7) | –(2.6) |
| | $Extent_2$ | +(23.8) | +(90.0) | +(66.2) | +(7.7) | –(39.1) |
| | $Area_1$ | +(88.5) | +(97.1) | +(94.8) | +(48.9) | +(71.1) |
| | $Area_2$ | +(43.7) | +(91.3) | +(83.6) | –(16.2) | –(15.4) |
| | $OW_1$ | –(94.2) | +(48.6) | –(99.5) | –(65.9) | –(93.3) |
| | $OW_2$ | –(31.0) | +(55.5) | –(80.7) | +(66.9) | –(58.5) |
| Indian Ocean | $Extent_1$ | +(63.5) | +(65.9) | +(34.0) | +(16.7) | +(87.1) |
| | $Extent_2$ | +(30.9) | +(64.1) | +(28.7) | –(6.4) | +(53.4) |
| | $Area_1$ | +(88.9) | +(93.2) | +(68.6) | +(85.1) | +(86.1) |
| | $Area_2$ | +(32.3) | +(78.8) | +(41.3) | +(30.3) | +(7.4) |
| | $OW_1$ | –(99.4) | –(58.8) | –(96.1) | –(100.0) | +(75.0) |
| | $OW_2$ | +(16.7) | +(21.8) | –(27.8) | –(91.7) | +(98.5) |
| West Pacific Ocean | $Extent_1$ | +(33.1) | +(74.8) | +(93.4) | +(13.1) | –(40.1) |
| | $Extent_2$ | –(5.5) | +(62.1) | +(89.3) | –(6.5) | –(72.6) |
| | $Area_1$ | +(94.0) | +(94.5) | +(99.5) | +(72.5) | +(54.0) |
| | $Area_2$ | +(50.2) | +(81.9) | +(96.1) | +(20.1) | –(32.8) |
| | $OW_1$ | –(99.6) | –(88.1) | –(99.3) | –(98.7) | –(97.6) |
| | $OW_2$ | –(91.4) | –(27.1) | –(51.9) | –(74.9) | –(94.0) |
| Ross Sea | $Extent_1$ | +(90.5) | +(90.6) | +(36.5) | +(49.9) | +(97.3) |
| | $Extent_2$ | +(83.9) | +(81.3) | +(33.2) | +(37.9) | +(94.5) |
| | $Area_1$ | +(95.7) | +(92.0) | +(66.8) | +(76.4) | +(98.8) |
| | $Area_2$ | +(72.3) | +(76.1) | +(39.7) | +(16.9) | +(87.6) |
| | $OW_1$ | +(11.1) | +(78.1) | –(88.1) | –(83.7) | +(30.0) |
| | $OW_2$ | +(92.8) | +(78.5) | –(5.5) | +(66.3) | +(96.5) |
| Amundsen Sea | $Extent_1$ | –(77.0) | –(99.2) | –(64.2) | +(8.8) | –(28.9) |
| | $Extent_2$ | –(83.6) | –(99.2) | –(70.1) | –(3.8) | –(45.4) |
| | $Area_1$ | –(30.3) | –(96.2) | –(13.1) | +(52.1) | –(18.4) |
| | $Area_2$ | –(70.1) | –(97.8) | –(47.1) | +(13.2) | –(59.7) |
| | $OW_1$ | –(99.7) | –(92.7) | –(99.7) | –(98.4) | –(42.1) |
| | $OW_1$ | –(95.9) | –(91.2) | –(97.4) | –(67.5) | +(7.4) |
| Bellingshausen Sea | $Extent_1$ | –(63.6) | –(99.8) | –(50.9) | –(20.8) | –(8.8) |
| | $Extent_2$ | –(81.4) | –(99.9) | –(74.3) | –(39.7) | –(33.7) |
| | $Area_1$ | –(60.6) | –(99.9) | –(45.4) | –(9.0) | –(6.0) |
| | $Area_2$ | –(86.2) | –(99.9) | –(79.3) | –(44.4) | –(49.5) |
| | $OW_1$ | –(68.1) | –(83.9) | –(56.2) | –(49.6) | –(12.8) |
| | $OW_2$ | –(63.4) | –(91.0) | –(60.1) | –(24.6) | –(3.2) |

Table II

Linear regression statistics of trends in total and regional Southern Ocean annual and seasonal sea ice extent, sea ice area and open water area. Only those trends which had 80% or greater $F$-test confidence levels in both the original (1) and GSFC reanalyzed (2) time-series, or which had at least a 90% $F$-test in the reanalyzed time-series, are reported here

| Region | Season | Ice index | Slope[a] | Std.[b] error | $F$-test (%) | Trend[b] (%) | GSFC corr.[c] |
|---|---|---|---|---|---|---|---|
| Southern Ocean | Summer | $Extent_1$ | +0.113 | 0.044 | 97.9 | +13.8 ± 5.4 | 1.00 |
| | | $Extent_2$ | +0.066 | 0.048 | 81.1 | +9.2 ± 6.7 | 0.99 |
| | Summer | $Area_1$ | +0.108 | 0.034 | 99.4 | +22.2 ± 7.0 | 0.98 |
| | | $Area_2$ | +0.051 | 0.035 | 82.9 | +11.7 ± 8.1 | 0.96 |
| | Autumn | $Area_1$ | +0.173 | 0.062 | 98.7 | +12.7 ± 4.6 | 0.96 |
| | | $Area_2$ | +0.091 | 0.064 | 82.1 | +6.9 ± 4.9 | 0.93 |
| | Autumn | $OW_1$ | –0.096 | 0.010 | 100.0 | –18.1 ± 1.9 | 0.90 |
| | | $OW_2$ | –0.037 | 0.012 | 99.6 | –7.0 ± 2.0 | 0.78 |
| Weddell | Summer | $Extent_1$ | +0.089 | 0.040 | 95.7 | +30.7 ± 13.9 | 1.00 |
| | | $Extent_2$ | +0.072 | 0.041 | 90.0 | +27.1 ± 15.4 | 1.00 |
| | Summer | $Area_1$ | +0.079 | 0.033 | 97.1 | +40.2 ± 16.6 | 0.99 |
| | | $Area_2$ | +0.059 | 0.032 | 91.3 | +32.3 ± 17.7 | 0.98 |
| | Autumn | $Area_1$ | +0.077 | 0.037 | 94.8 | +14.9 ± 7.1 | 0.99 |
| | | $Area_2$ | +0.053 | 0.036 | 83.6 | +10.4 ± 7.1 | 0.99 |
| | Autumn | $OW_1$ | –0.032 | 0.010 | 99.5 | –20.5 ± 6.2 | 0.90 |
| | | $OW_2$ | –0.015 | 0.011 | 80.7 | –9.2 ± 6.7 | 0.80 |
| Indian | Winter | $OW_1$ | –0.033 | 0.006 | 100.0 | –23.1 ± 4.3 | 0.64 |
| | | $OW_2$ | –0.012 | 0.006 | 91.7 | –8.5 ± 4.5 | 0.09 |
| | Spring | $OW_1$ | +0.009 | 0.007 | 75.0 | +4.8 ± 4.0 | 0.96 |
| | | $OW_2$ | +0.021 | 0.008 | 98.5 | +11.7 ± 4.2 | 0.87 |
| West Pacific | Annual | $OW_1$ | –0.070 | 0.020 | 99.6 | –20.5 ± 6.0 | 0.95 |
| | | $OW_2$ | –0.038 | 0.021 | 91.4 | –11.9 ± 6.4 | 0.94 |
| | Summer | $Area_1$ | +0.023 | 0.011 | 94.5 | +41.7 ± 20.0 | 0.99 |
| | | $Area_2$ | +0.016 | 0.012 | 81.9 | +35.0 ± 25.0 | 0.99 |
| | Autumn | $Extent_1$ | +0.026 | 0.013 | 93.4 | +12.5 ± 6.3 | 1.00 |
| | | $Extent_2$ | +0.024 | 0.014 | 89.3 | +12.4 ± 7.2 | 1.00 |
| | Autumn | $Area_1$ | +0.039 | 0.012 | 99.5 | +28.7 ± 8.6 | 0.99 |
| | | $Area_2$ | +0.027 | 0.012 | 96.1 | +21.3 ± 9.4 | 0.98 |
| | Spring | $OW_1$ | –0.029 | 0.011 | 97.6 | –27.8 ± 11.0 | 0.97 |
| | | $OW_2$ | –0.024 | 0.012 | 94.0 | –24.4 ± 11.9 | 0.95 |
| Ross | Annual | $Extent_1$ | +0.227 | 0.127 | 90.5 | +10.6 ± 5.9 | 1.00 |
| | | $Extent_2$ | +0.181 | 0.123 | 83.9 | +8.7 ± 5.9 | 1.00 |
| | Annual | $OW_1$ | +0.006 | 0.039 | 11.1 | +1.0 ± 6.9 | 0.90 |
| | | $OW_2$ | +0.072 | 0.037 | 92.8 | +12.9 ± 6.6 | 0.86 |
| | Summer | $Extent_1$ | +0.065 | 0.036 | 90.6 | +31.7 ± 17.7 | 1.00 |
| | | $Extent_2$ | +0.049 | 0.036 | 81.3 | +26.6 ± 19.2 | 0.99 |
| | Spring | $Extent_1$ | +0.096 | 0.039 | 97.3 | +14.7 ± 6.0 | 1.00 |
| | | $Extent_2$ | +0.079 | 0.038 | 94.5 | +12.3 ± 5.9 | 0.99 |

Table II
*(Continued)*

| Region | Season | Ice index | Slope[a] | Std.[b] error | $F$-test (%) | Trend[b] (%) | GSFC corr.[c] |
|---|---|---|---|---|---|---|---|
| | Spring | $Area_1$ | +0.091 | 0.031 | 98.8 | +18.9 ± 6.5 | 0.99 |
| | | $Area_2$ | +0.050 | 0.030 | 87.6 | +10.7 ± 6.6 | 0.99 |
| | Spring | $OW_1$ | +0.005 | 0.013 | 30.0 | +3.0 ± 7.6 | 0.98 |
| | | $OW_2$ | +0.029 | 0.012 | 96.5 | +16.6 ± 7.1 | 0.97 |
| Amundsen | Annual | $OW_1$ | –0.058 | 0.016 | 99.7 | –25.2 ± 6.9 | 0.93 |
| | | $OW_2$ | –0.035 | 0.016 | 95.9 | –15.4 ± 6.8 | 0.91 |
| | Summer | $Extent_1$ | –0.036 | 0.012 | 99.2 | –37.6 ± 12.3 | 1.00 |
| | | $Extent_2$ | –0.039 | 0.013 | 99.2 | –44.1 ± 14.5 | 0.99 |
| | Summer | $Area_1$ | –0.022 | 0.010 | 96.2 | –39.0 ± 17.1 | 0.99 |
| | | $Area_2$ | –0.027 | 0.011 | 97.8 | –50.8 ± 20.0 | 0.99 |
| | Summer | $OW_1$ | –0.013 | 0.007 | 92.7 | –35.4 ± 18.4 | 0.97 |
| | | $OW_2$ | –0.012 | 0.006 | 91.2 | –33.8 ± 18.6 | 0.98 |
| | Autumn | $OW_1$ | –0.017 | 0.006 | 99.7 | –30.6 ± 8.6 | 0.52 |
| | | $OW_2$ | –0.011 | 0.004 | 97.4 | –20.2 ± 8.2 | 0.40 |
| Bellingshausen | Summer | $Extent_1$ | –0.032 | 0.009 | 99.8 | –57.9 ± 15.9 | 1.00 |
| | | $Extent_2$ | –0.042 | 0.011 | 99.9 | –95.8 ± 24.7 | 0.99 |
| | Summer | $Area_1$ | –0.028 | 0.007 | 99.9 | –89.4 ± 22.7 | 1.00 |
| | | $Area_2$ | –0.034 | 0.078 | 99.9 | –127.3 ± 28.9 | 0.99 |
| | Summer | $OW_1$ | –0.004 | 0.003 | 83.9 | –17.5 ± 11.9 | 0.99 |
| | | $OW_2$ | –0.007 | 0.004 | 91.0 | –43.5 ± 24.0 | 0.96 |

[a] Units: $10^6$ $km^2$/yr.
[b] Trend determined by multiplying the slope and standard error by the number of years and by 100 then dividing by the mean of the time series in question.
[c] Correlation between GSFC and the original NASA Team derived time-series for the period of overlap (7/87–8/95).

In order to capture information on the seasonal timing and magnitude of sea ice extent, sea ice area and open water area, seasonal time-series were created. These time-series were determined by integrating regional and total Southern Ocean sea ice extent, sea ice area and open water area for (i) summer (Jan–Mar), (ii) autumn (Apr–Jun), (iii) winter (Jul–Sep), and (iv) spring (Oct–Dec). Because the data period is from November 1978 to August 1995, the summer and autumn time-series have 17 years, whereas the winter and spring time-series have 16 years. The analysis of the original time-series of Southern Ocean seasonal sea ice coverage shows detectable increasing trends in summer sea ice extent and area, in autumn, winter and spring sea ice area, and decreasing trends in autumn, winter and spring open water area. In the GSFC reanalyzed time-series the summer sea ice extent and area and autumn sea ice area trends are just below the designated detection level ($F$-test less than 90% but greater than 80%), and the only trend above the 90% detection level is the autumn open water area. Figure 3 shows the four seasonal

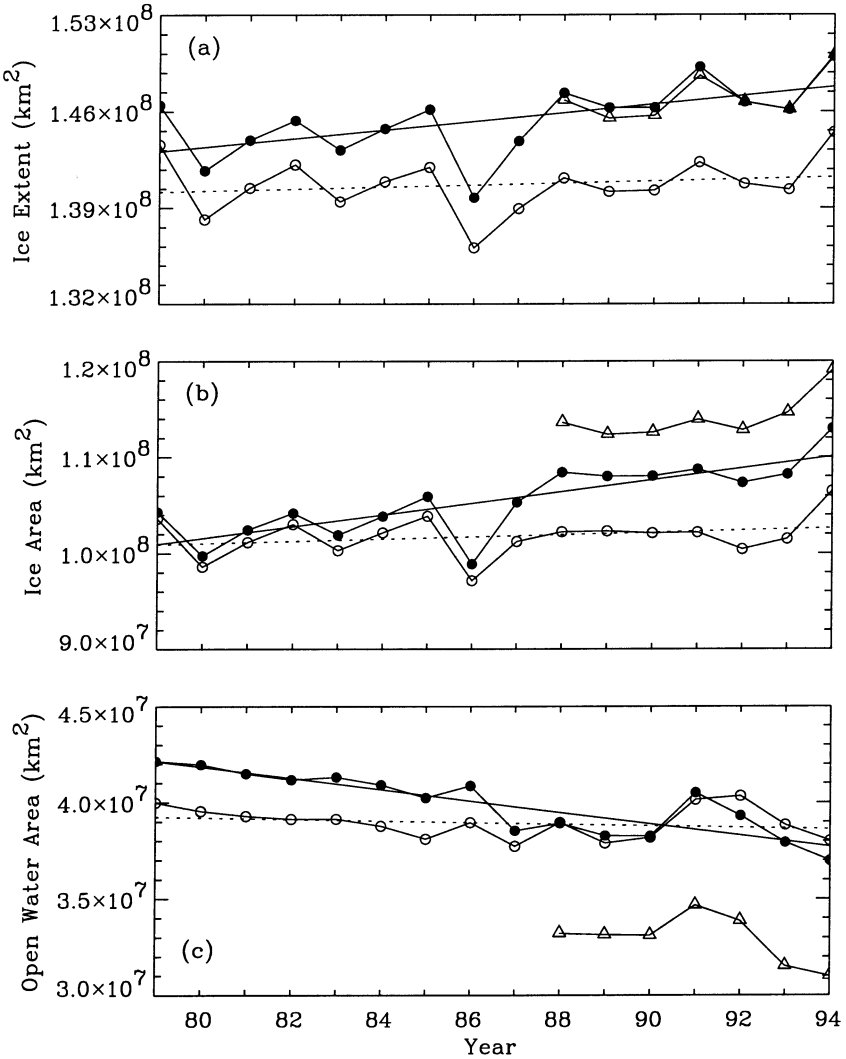


*Figure 2.* Southern Ocean annual integrated sea ice coverage from 1979 to 1994 for: (a) sea ice extent, (b) sea ice area, and (c) open water area inside the boundary of sea ice extent. The closed and open circles indicate the original and GSFC reanalyzed NASA Team derived sea ice concentrations, respectively; the open triangles indicate GSFC Bootstrap derived sea ice concentrations for the period of overlap (1988–1994). The solid and dotted lines are the linear least-squares regressions for the original and GSFC reanalyzed time-series, respectively. See Tables I and II for linear regression statistics.

time-series determined for total Southern Ocean sea ice area. As indicated by the regressions, the original and GSFC reanalyzed time-series do not depart as significantly in the summer and autumn time-series as in the winter and spring time-series.

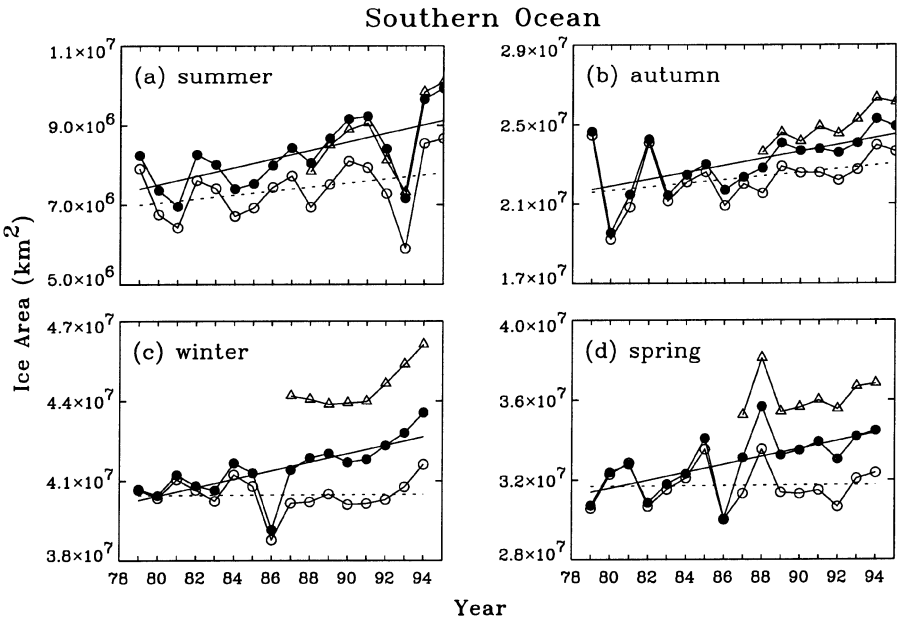


*Figure 3.* Southern Ocean seasonal integrated sea ice area. Symbols and lines are the same as in Figure 2. See Tables I and II for linear regression statistics.

The linear regression results reported for the regional seasonal time-series tabulated in Table I, as well as the seasonal time-series plots of sea icea area for all 6 regions (Figures 4–9), show which *regions* were contributing to the trends observed in total Southern Ocean seasonal sea ice coverage. (Figures of seasonal sea ice extent and open water area can be found in Stammerjohn et al., 1997.) Of the thirty-three detectable trends reported in the original analysis of the regional seasonal time-series, thirteen remain detectable in the GSFC reanalyzed time-series, nine are just under the designated detection level ($F$-test less than 90% but greater than 80%), and three have detectable trends which were not detectable in the original analysis. However, what is most notable about the regional seasonal analysis, which is best illustrated in Table I, is the general opposition in trends between the two southeastern Pacific regions (the Amundsen and Bellingshausen) and the other four regions, an observation supported by both the original and GSFC reanalyzed time-series. The Amundsen and Bellingshausen (AB) regions show decreasing trends in sea ice extent, sea ice area and open water area (most significantly in summer), whereas the other four regions in general show increasing trends in sea ice extent and area (most significantly in non-winter seasons) but, for most regions, decreasing trends in open water area (notable exceptions are the detectable increasing trends in Indian spring and Ross annual and spring open water areas). Whatever the causative factors influencing these trends, they appear to be strongest in non-

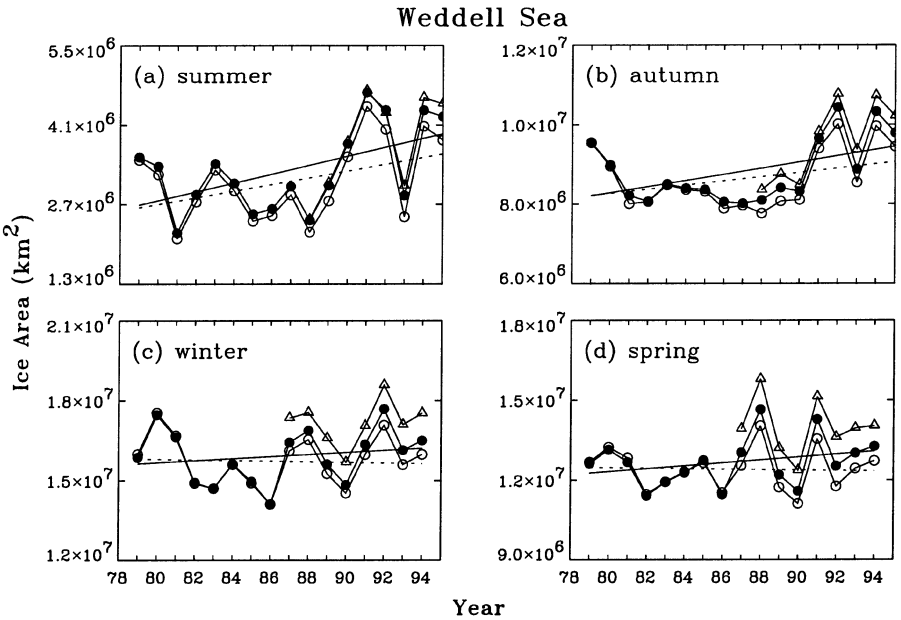


*Figure 4.* Weddell Sea seasonal integrated sea ice area. Symbols and lines are the same as in Figure 2. See Tables I and II for linear regression statistics.

winter months, since none of the *regional* time-series show detectable trends in winter sea ice extent or area.

## 3. Other Evidence of Contrasting Climate Patterns

Analyses of both the original and GSFC reanalyzed 16.8 year annual and seasonal time-series of Southern Ocean regional sea ice coverage show: (i) variability in trends with respect to season, where trends are most detectable in non-winter months, and (ii) variability in trends with respect to region, where a persistent opposition exists between decreasing summer sea ice and open water area in the AB regions versus increasing sea ice coverage in non-winter months everywhere else in the Southern Ocean. How does this 16.8 year record relate to other longer term climatic records? Are these increasing/decreasing trends in sea ice coverage during non-winter months indicative of a climate trend, and if so, why the asymmetric response? Is the asymmetry due to differential response times between atmospheric and oceanic forcing on sea ice coverage, or to persistent regional climate patterns?

It is first important to consider these results within the context of the satellite data used. These data are the product of three successive passive microwave sensors, with different frequencies, footprint sizes, visit times and calibrations. In order to assure both accuracy and consistency for long-term observations, the records from the successive passive microwave sensors must be carefully merged, as noted by

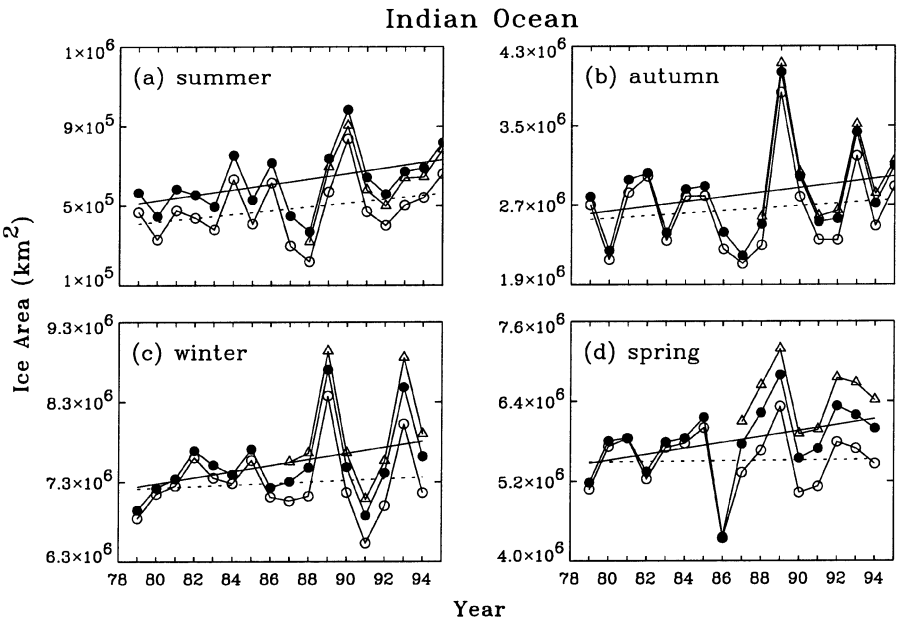


*Figure 5.* Indian Ocean seasonal integrated sea ice area. Symbols and lines are the same as in Figure 2. See Tables I and II for linear regression statistics.

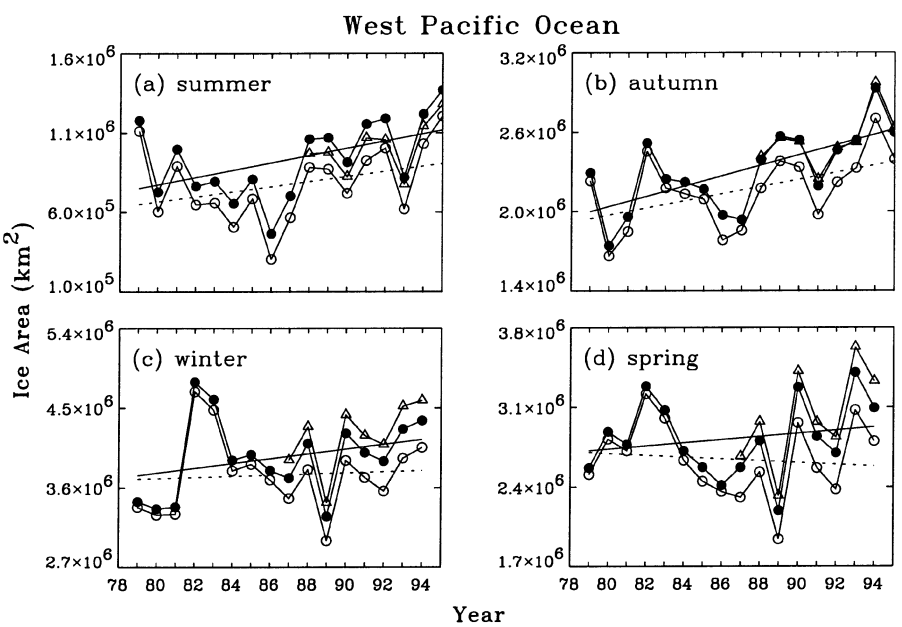


*Figure 6.* West Pacific Ocean seasonal integrated sea ice area. Symbols and lines are the same as in Figure 2. See Tables I and II for linear regression statistics.

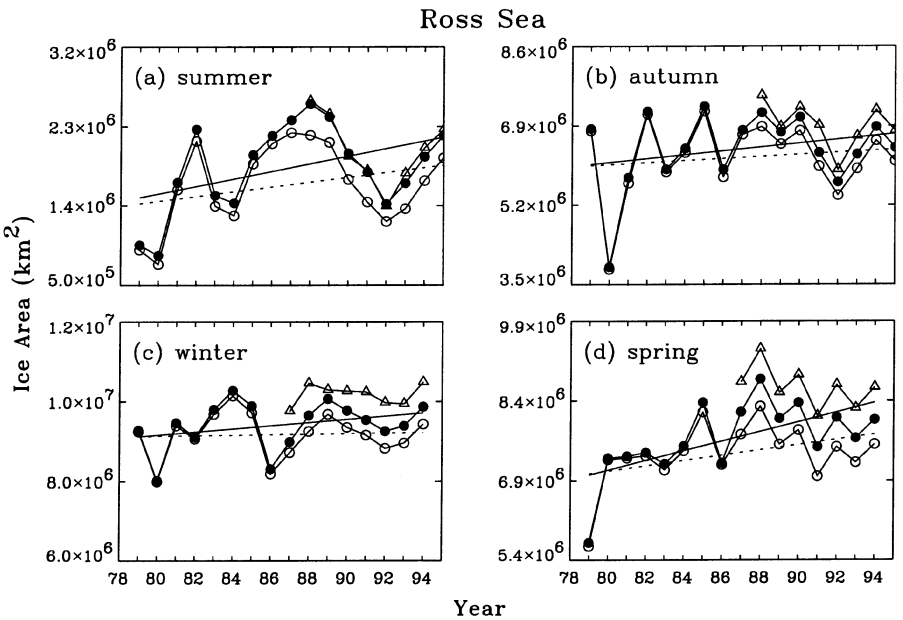


*Figure 7.* Ross Sea seasonal integrated sea ice area. Symbols and lines are the same as in Figure 2. See Tables I and II for linear regression statistics.

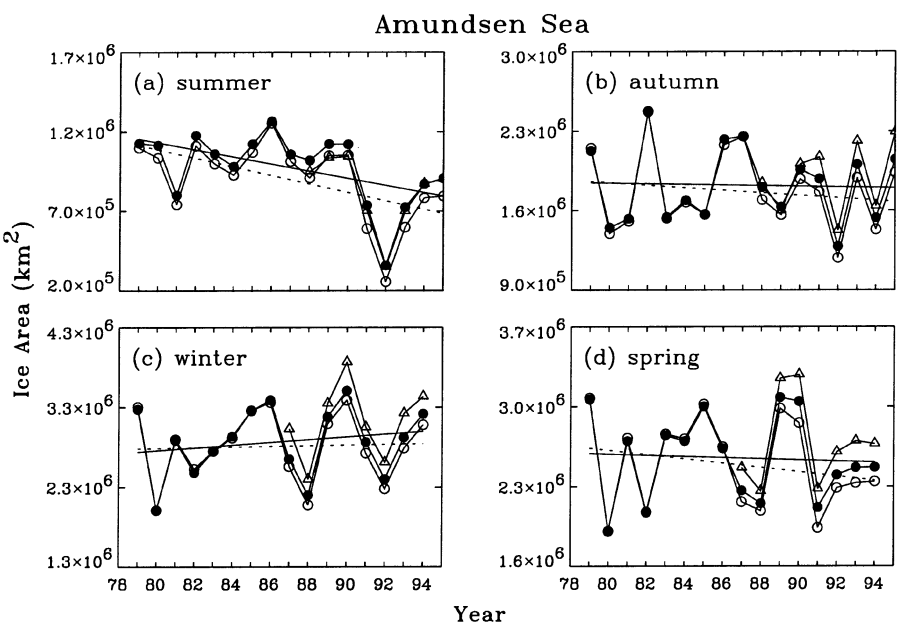


*Figure 8.* Amundsen Sea seasonal integrated sea ice area. Symbols and lines are the same as in Figure 2. See Tables I and II for linear regression statistics.

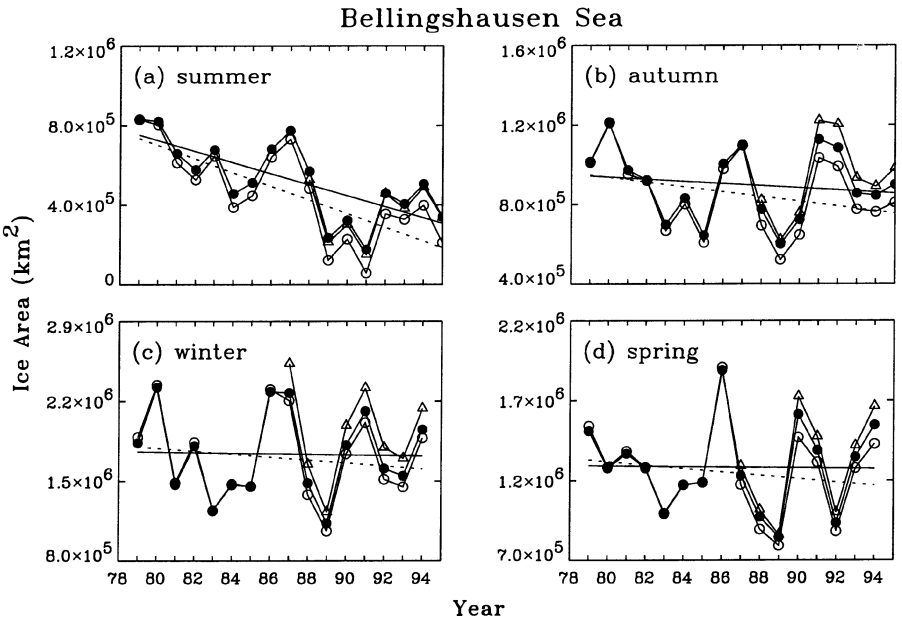


*Figure 9.* Bellingshausen Sea seasonal integrated sea ice area. Symbols and lines are the same as in Figure 2. See Tables I and II for linear regression statistics.

several other researchers (Cavalieri et al., 1997; Stroeve et al., 1997; Bjørgo et al., 1997; Abdalati et al., 1995; Wentz, 1995; Zabel and Jezek, 1994; Jezek et al., 1991). The GSFC reanalysis makes several important corrections in order to achieve this, one of which is the intersensor calibration which appears to make the biggest impact on the observed trends in Southern Ocean sea ice coverage (as compared to the original, less rigorously corrected time-series). Results from the GSFC reanalyzed data show that for total Southern Ocean sea ice extent, the 8 year SSM/I derived data have been adjusted down significantly so that the strong increasing trend observed in the original time-series (Figures 2–3) has been reduced. Although the pattern of positive trends observed everywhere but in the AB regions still holds true in the reanalysis, in general the strength of many of the increasing trends has been reduced below the 90% detection level. Nonetheless, there are still detectable increasing trends for some regions and some seasons (most notably in Weddell summer sea ice extent and area, West Pacific autumn sea ice area and Ross spring sea ice extent). Further, the decreasing trends in summer sea ice extent, sea ice area and open water area are still very strong in the AB regions.

We therefore have presented results from the original and the GSFC reanalyzed time-series in order to illustrate the differences and bring awareness of the caveats involved in merging the records from the successive passive microwave sensors. Applying an intersensor correction to the 16.8 year passive microwave data, as applied in the GSFC reanalysis, is problematic because it will be based on very

short overlap periods (2–3 weeks) which include seasonal biases as well. There is also the issue that recent comparisons of the SSM/I F11 and F13 (the latest SSM/I sensor) brightness temperature data, which overlap for a considerably longer period (May to September 1995), show a relation which is highly sensitive to the region chosen for comparison, suggesting that a hemisphere calibration of the two sensors will not satisfactorily improve the differences in sea ice extent and area (Stroeve et al., 1997). Finally, as the passive microwave record becomes longer, it is very possible that advances in technology and experimental protocols may improve observation precision and accuracy (Zabel and Jezek, 1994). However, how these improvements are incorporated into the merged sensor data and how they impact the consistency of the time-series will remain an issue. It is also possible that these improvements may result in further reanalysis of the passive microwave data, consequently impacting our interpretation of the trend patterns once more. With these caveats in mind, we feel that the GSFC reanalyzed time-series is a conservative measure of the sea ice variability in the Southern Ocean, so that the contrasting pattern of positive versus negative trends, which remains evident even in the rigorous GSFC reanalysis, is a real feature of the Antarctic, although as yet little understood. We therefore explore other evidence which supports this observation and which may indicate what forcing mechanisms may be contributing to its existence.

The zonal non-uniformity of circumpolar sea ice extent anomalies is a well characterized feature of the Southern Ocean (Zwally et al., 1983b; Parkinson, 1992; Gloersen et al., 1992; Parkinson, 1994). As a consequence, it would not be surprising to observe asymmetry between sea ice anomalies in the AB regions versus the rest of the Southern Ocean over a year or two period. However, it is noteworthy that not only has the asymmetry been maintained over a 16.8 year record, but that it reveals detectable opposing trends in sea ice coverage. Jacobs and Comiso (1993) reported a record decrease in Bellingshausen (62–100° W) sea ice extent from mid-1988 through early 1991 which was most evident in the summer perennial sea ice extent. They show that this decrease coincided with (i) an increase in northwest surface winds (which would explain the concurrent decrease in open water area observed here), (ii) an increase in cyclonic activity, and (iii) a rise in surface air temperatures in the western Antarctic Peninsula region. More recently, Jacobs and Comiso (1997) show that this record decrease they observed in the Bellingshausen from mid-1988 through early 1991 was part of a long-term decline in sea ice extent of about 20% in both the Amundsen (100–130° W) and Bellingshausen Seas from 1973 to 1993. They show that this overall decline correlates with an increase in surface air temperature on the west side of the Antarctic Peninsula, which, as reported by many (King, 1994; Stark, 1994; Smith et al., 1996; Jacobs and Comiso, 1997), has been increasing at about 0.05–0.06 °C per year since the mid-1940's. They suggest that the decline observed in Amundsen and Bellingshausen sea ice extents may indicate a response to larger-scale atmospheric circulation changes in the southeastern Pacific, in addition to changes in regional

oceanic circulation (such as a weakening of surface currents and/or an increase in upwelling of Circumpolar Deep Water on the continental shelf). Finally, Jacobs and Comiso (1993, 1997) mention that these findings are inconsistent with global warming models (Stouffer et al., 1989; Manabe et al., 1991) which predict a fresher surface layer and thicker sea ice cover. If these trends are a result of global warming, could it be that it has a two-fold effect in the Southern Ocean, whereby all regions are experiencing colder conditions except the southeastern Pacific region which is experiencing warmer conditions?

There is evidence in other studies of similar patterns in regional climate variables. For example, a recurring opposition in air temperature anomalies between Antarctic Peninsula and mainland stations has been observed in all seasons but spring (Rogers, 1983). Rogers shows that temperature variability in solstitial seasons is associated with zonal flow, while in equinoctial seasons it is associated with meridional circulation. During solstice seasons when the westerlies are unusually strong (weak), temperatures at mainland stations are colder (warmer), while temperatures at peninsula stations are warmer (colder). Unusually warm (cold) temperatures also are observed at peninsula stations during autumn and winter when the trough across New Zealand is weak (strong), but during *spring* when the mean ridge across New Zealand is weak (strong), warmer (colder) temperatures are experienced in the peninsula sector. The mainland stations in Rogers' study were comprised mostly of coastal stations in the Weddell, Indian, West Pacific and Ross regions, so that the Amundsen region was not specifically represented. The Bellingshausen region was represented by the peninsula stations which were comprised mostly of stations on the western side of the Antarctica Peninsula.

The belt of strongest westerlies, as approximated by 500 mb geostrophic wind exceeding 20 m/s, is typically confined to the zonal region east of the Antarctic Peninsula to about 180° E, so that with the exception of the AB regions, most of the Southern Ocean is in close proximity to this belt of strong westerlies (van Loon et al., 1971; Trenberth, 1981; Rogers, 1983). Fluctuations in the southern hemisphere high latitude 500 mb zonal flow have been associated with the asymmetries of the Antarctic continent and the sea surface temperature differences in the surrounding waters (van Loon and Jenne, 1972; Trenberth, 1980). Decadal shifts in the 500 mb flow have been observed between the 1960's and 1970's (Trenberth, 1980) and between the 1970's and 1980's, of which the latter also coincided with an increase in the westerlies in the late 1970's and 1980's (Trenberth, 1984; van Loon et al., 1993; Hurrell and van Loon, 1994). Trenberth (1984) showed that the year 1979, the year of the Global Weather Experiment, was characterized by an exceptionally deep Antarctic circumpolar trough and increased westerlies south of 45° with a concurrent decrease of the westerlies north of 45°, indicating a southward shift in the main westerly jet in summer and enhanced polar jet in winter. Other studies showed an overall increase in the westerlies during the 1980's as compared to the 1970's, presumably due to a modulation of the southern hemisphere atmospheric cycle (Trenberth, 1980; van Loon et al., 1993; Hurrell and

van Loon, 1994). According to these studies, the semi-annual oscillation (SAO) of sea level pressure which typically involves minima over middle latitudes during solstitial seasons and minima over higher latitudes (south of 60°) during equinoctial seasons, weakened in the 1980's as compared to the 1970's, suggesting that the movement and intensity of the circumpolar trough changed significantly. This resulted in lower pressure poleward in the circumpolar trough during late spring and summer when usually the trough moves equatorward. The lower pressures are accompanied by stronger winds, thus enhancing the westerlies in late spring and summer which, following the observations by Rogers (1983), would promote colder continental temperatures and warmer peninsula temperatures. Finally, there have been other observations showing that in years of enhanced poleward heat transport, the position of the sub-tropical high pressure belt is shifted further north in winter and spring (Pittock, 1973). Pittock associated the increase in the poleward transport of heat with an increase in the strength of the Hadley circulation, but Trenberth (1975) associated it with an increase in the meridional transport by large-scale eddies.

Further evidence of contrasting climate patterns in Antarctica comes from a paleo-environmental study (Mosley-Thompson et al., 1990; Mosley-Thompson, 1995). Ice cores were collected from Siple Station (near the Antarctic peninsula) and Amundsen–Scott Station (South Pole). Siple Station lies between the Antarctic Peninsula region and the polar plateau and is thought to be a sensitive indicator of the climate transition between the cold dry conditions of the continent and the maritime conditions of the western Antarctic Peninsula region (Mosley-Thompson et al., 1990). Oxygen isotope and dust particle information extracted from the cores suggests that during much of the last five centuries warmer, less dusty atmospheric conditions prevailed at Siple while colder, more dusty atmospheric conditions prevailed at the South Pole. These results compare well with the opposition found by Rogers (1983) and suggests that a prolonged period of intensified westerlies promoted the warm peninsula versus cold continental regional climates. The opposition in dust concentrations also may indicate different transport pathways from lower latitudes. During intensified westerlies more material may be entrained higher into the atmosphere at lower latitudes and subsequently carried south and deposited (Mosley–Thompson et al., 1990). This is in agreement with observations of the terrestrial component of the aerosol mass at the South Pole which are believed to be associated with an upper tropospheric or lower stratospheric source (Hogan et al., 1984). In contrast, storms are more frequent and severe in the Siple and western Antarctic Peninsula region, so that material transport here has a lower tropospheric pathway. The precipitation carried with these storms is also an efficient mechanism for removing entrained dust so that the air reaching Siple would be very clean (Hogan, 1975), an observation supported by microparticle analyses (Mosley-Thompson et al., 1990).

Does the intensification of the westerlies lead to colder temperatures on the polar plateau or do the colder temperatures promote the intensification of the westerlies?

Based on results of general circulation models, it would seem that the former is the case (Stouffer et al., 1989; Manabe et al., 1991, 1992; Manabe and Stouffer, 1996). According to these studies, with a doubling of atmospheric $CO_2$ and consequent increase in surface air temperature, a coupled ocean–atmosphere general circulation model predicts little warming in the circumpolar ocean of the southern hemisphere due to vertical mixing of heat over a deep water column with large heat capacity. There is a freshening of surface waters due to increased precipitation which weakens convective mixing, lowering sea surface temperature. This in turn increases the meridional temperature gradient, causing the westerlies to intensify, promoting equatorward Ekman drift of surface waters and reducing the poleward transport of heat. In those regions within the belt of strong westerlies, these conditions would promote decreased air temperatures and increased ice growth.

The regional circulation features of the Southern Ocean have not yet been well identified, thus it is difficult to determine what is contributing to the opposing trends in Southern Ocean regional ice coverage observed here. However, the temporal trends and spatial patterns found in the 16.8 year record of Southern Ocean sea ice coverage appear to have existed before, if not always. Perhaps the increase in sea ice coverage observed everywhere in the Southern Ocean except in the AB regions for the 1978–1995 period is part of a long-term increase in sea ice coverage first observed in the 1966 to 1972 record (Streten, 1973; Sissala et al., 1972; Zwally et al., 1983a). Or perhaps the decrease in Southern Ocean sea ice extent observed in the 1973–1980 record (Kukla and Garvin, 1981; Zwally et al., 1983a) suggests that long-term variability in the Southern Ocean consists of short-term decadal fluctuations. Decadal shifts have been observed in the southern hemisphere atmospheric circulation between the 1960's to 1980's (Trenberth, 1979; van Loon et al., 1993). Finally, the paleo-environmental study of ice cores (Mosley-Thompson et al., 1990; Mosley-Thompson, 1995) suggests that regardless of the temporal fluctuations, the spatial contrasting climate patterns in the Southern Ocean have been persistent features over much of the last five centuries.

The nature of these trends in Southern Ocean sea coverage would be better understood if we could identify the climate patterns forcing these trends, thereby bringing to use the longer meteorological records. One wonders whether the ENSO signals detected in Southern Ocean sea ice coverage contribute to the trends observed here, or do they contribute more to shorter term fluctuations which are superimposed on these longer term trends? Since ENSO signals are strongest in the southeastern Pacific region (Trenberth, 1981; White and Peterson, 1996) and have been clearly detected in western Antarctic Peninsula sea ice coverage (Smith et al., 1996), they may play a role in the climate pattern affecting the opposition observed between the AB region and the rest of the Southern Ocean. It is clear, however, that such an opposition of climate patterns in the Southern Ocean impacts our understanding of regional and global oceanic and atmospheric circulation and consequently, global change scenarios, and a complete understanding of what is causing the persistence in these regional sea ice trends awaits further study.

## Acknowledgements

We thank the National Snow and Ice Data Center (Boulder, Colorado), who made available both the original and GSFC reanalyzed 16.8 year NASA Team derived sea ice concentration data, and J. C. Comiso, who made available SSM/I tie-points for the determination of GSFC Bootstrap derived sea ice concentrations for the 1987–1995 period. This work was funded by National Science Foundation grant DPP90-11927.

## References

Abdalati, W., Steffen, K., Otto, C., and Jezek, K.: 1995, 'Comparison of Brightness Temperatures from SSM/I Instruments on the DMSP F8 and F11 Satellites for Antarctica and Greenland Ice Sheet', *Int. J. Remote Sens.* **16**, 1223–1229.

Ainley, D. G., Ribic, C. A., and Fraser, W. R.: 1994, 'Ecological Structure Among Migrant and Resident Seabirds of the Scotia–Weddell Confluence Region', *J. Animal Ecol.* **63**, 347–364.

Bjørgo, E., Johannessen, O. M., and Miles, M. W.: 1997, 'Analysis of Merged SMMR-SSMI Time Series of Arctic and Antarctic Sea Ice Parameters 1978–1995', *Geophys. Res. Lett.* **24**, 413–416.

Budd, W. F.: 1975, 'Antarctic Sea-Ice Variations from Satellite Sensing in Relation to Climate', *J. Glaciol.* **15**, 417–427.

Carleton, A. M.: 1989, 'Antarctic Sea-Ice Relationships with Indices of the Atmospheric Circulation of the Southern Hemisphere', *Clim. Dynam.* **3**, 207–220.

Cavalieri, D. J., Campbell, W. J., and Gloersen, P.: 1984, 'Determination of Sea Ice Parameters with the NIMBUS 7 SMMR', *J. Geophys. Res.* **89**, 5355–5369.

Cavalieri, D. J., St. Germain, K. M., and Swift, C. T.: 1995, 'Reduction of Weather Effects in the Calculation of Sea-Ice Concentration with the DMSP SSM/I', *J. Glaciol.* **41**, 455–464.

Cavalieri, D. J., Parkinson, C. L., Gloersen, P., and Zwally, H. J.: 1997, 'Arctic and Antarctic Sea Ice Concentrations from Multichannel Passive-Microwave Satellite Data Sets: October 1978 to September 1995, User's Guide', *NASA Technical Memorandum 104647*, 17 pp.

Comiso, J. C.: 1983, 'Sea Ice Effective Microwave Emissivities from Satellite Passive Microwave and Infrared Observations', *J. Geophys. Res.* **88**, 7686–7704.

Comiso, J. C.: 1995, *SSM/I Sea Ice Concentrations Using the Bootstrap Algorithm, (NASA RP-1380)*, National Aeronautics and Space Administration, Washington, D.C., 49 pp.

Comiso, J. C., Ackley, S. F., and Gordon, A. L.: 1984, 'Antarctic Sea Ice Microwave Signatures and Their Correlation with In Situ Ice Observations', *J. Geophys. Res.* **89**, 662–672.

Comiso, J. C., Grenfell, T. C., Lange, M., Lohanick, A. W., Moore, R. K., and Wadhams, P.: 1992, 'Microwave Remote Sensing of the Southern Ocean Ice Cover', in Carsey, F. D. (ed.), *Microwave Remote Sensing of Sea Ice*, American Geophysical Union, Washington, D.C., pp. 243–259.

Comiso, J. C., Cavalieri, D., Parkinson, C., and Gloersen, P.: 1997, 'Passive Microwave Algorithms for Sea Ice Concentration – A Comparison of Two Techniques', *Rem. Sens. Envir.* **60**, 357–384.

Durbin, J. and Watson, G. S.: 1971, 'Testing for Serial Correlation in Least Squares Regression, III', *Biometrika* **58**, 1–19.

Emery, W. J., Fowler, C., and Maslanik, J.: 1994, 'Arctic Sea Ice Concentrations from Special Sensor Microwave Imager and Advanced Very High Resolution Radiometer Satellite Data', *J. Geophys. Res.* **99**, 18,329–18,342.

Fletcher, J. O.: 1969, 'Ice Extent on the Southern Ocean and Its Relation to World Climate', *Rand Corporation Research Memorandum RM-5793-NSF*, Rand Corporation, Santa Monica, California 90406.

Fletcher, J. O., Radok, U., and Slutz, R.: 1982, 'Climatic Signals of the Antarctic Ocean', *J. Geophys. Res.* **87**, 4269–4276.

Fraser, W. R., Trivelpiece, W. Z., Ainley, D. G., and Trivelpiece, S. G.: 1992, 'Increases in Antarctic Penguin Populations: Reduced Competition with Whale or a Loss of Sea Ice Due to Environmental Warming?', *Polar Biol.* **11**, 525–531.

Gloersen, P.: 1995, 'Modulation of Hemispheric Sea-Ice Cover by ENSO Events', *Nature* **373**, 503–506.

Gloersen, P. and Campbell, W. J.: 1991, 'Recent Variations in Arctic and Antarctic Sea-Ice Covers', *Nature* **352**, 33–36.

Gloersen, P. and Cavalieri, D. J.: 1986, 'Reduction of Weather Effects in the Calculation of Sea Ice Concentrations from Microwave Radiances', *J. Geophys. Res.* **91**, 3913–3919.

Gloersen, P., Campbell, W. J., Cavalieri, D. J., Comiso, J. C., Parkinson, C. L., and Zwally, H. J.: 1992, *Arctic and Antarctic Sea Ice, 1978–1987: Satellite Passive-Microwave Observations and Analysis, (NASA SP-511)*, National Aeronautics and Space Administration, Washington, D.C., 290 pp.

Hogan, A. W.: 1975, 'Antarctic Aerosols', *J. Appl. Meteorol.* **14**, 550–559.

Hogan, A., Kebschull, K., Townsend, R., Murphey, B., Samson, J., and Barnard, S.: 1984, 'Particle Concentrations at the South Pole, on Meteorological and Climatological Time Scales; Is the Difference Important?', *Geophys. Res. Lett.* **11**, 850–853.

Hunt, G. L.: 1991, 'Marine Birds and Ice-Influenced Environments of Polar Oceans', *J. Marine Systems* **2**, 233–240.

Hurrell, J. W. and Loon, H. van: 1994, 'A Modulation of the Atmospheric Annual Cycle in the Southern Hemisphere', *Tellus* **46A**, 325–338.

Jacka, T. H.: 1990, 'Antarctic and Southern Ocean Sea-Ice and Climate Trends', *Ann. Glaciol.* **14**, 127–130.

Jacobs, S. S. and Comiso, J. C.: 1993, 'A Recent Sea-Ice-Retreat West of the Antarctic Peninsula', *Geophys. Res. Lett.* **20**, 1171–1174.

Jacobs, S. S. and Comiso, J. C.: 1997, 'Climate Variability in the Amundsen and Bellingshausen Seas', *J. Clim.* **10**, 697–709.

Jezek, K. C., Merry, C., Cavalieri, D., Grace, S., Bedner, J., Wilson, D., and Lampkin, D.: 1991, 'Comparison Between SMMR and SSM/I Passive Microwave Data Collected over the Antarctic Ice Sheet', *Byrd Polar Research Center Technical Report 91-03*, Ohio State University, Columbus.

King, J. C.: 1994, 'Recent Climate Variability in the Vicinity of the Antarctic Peninsula', *Int. J. Climatol.* **14**, 357–369.

Kukla, G. and Garvin, J.: 1981, 'Summer Ice and Carbon Dioxide', *Science* **214**, 497–503.

Manabe, S. and Stouffer, R. J.: 1996, 'Low-Frequency Variability of Surface Air Temperature in a 1000-Year Integration of a Coupled Atmosphere–Ocean–Land-Surface Model', *J. Clim.* **9**, 376–393.

Manabe, S., Stouffer, R. J., Spelman, M. J., and Bryan, K.: 1991, 'Transient Responses of a Coupled Ocean Atmosphere Model to Gradual Changes of Atmospheric $CO_2$. (1) Annual Mean Response', *J. Clim.* **4**, 785–818.

Manabe, S., Spelman, M. J., and Stouffer, R. J.: 1992, 'Transient Responses of a Coupled Ocean–Atmosphere Model to Gradual Changes of Atmospheric $CO_2$. (2) Seasonal Response', *J. Clim.* **5**, 105–126.

Martino, M. G., Cavalieri, D. J., Gloersen, P., and Zwally, H. J.: 1995, 'An Improved Land Mask for the SSM/I Grid', *NASA Technical Memorandum 104625*.

Mosley-Thompson, E.: 1995, 'Paleo-Environmental Conditions in Antarctica since 1500 A.D.: Ice Core Evidence', in Bradley, R. S. and Jones, P. D. (eds.), *Climate since 1500 A.D.*, Routledge, New York, pp. 572–591.

Mosley-Thompson, E., Thompson, L. G., Grootes, P. M., and Gundestrup, N.: 1990, 'Little Ice Age (Neoglacial) Paleo-Environmental Conditions at Siple Station, Antarctica', *Ann. Glaciol.* **14**, 199–204.

NSIDC: 1994, *Nimbus-7 SMMR Polar Radiances and Arctic and Antarctic Sea Ice Concentrations on CD-ROM User's Guide*, NSIDC Distributed Active Archive Center, University of Colorado at Boulder. Digital data available from nsidc@kryos.colorado.edu.

NSIDC: 1996, *DMSP SSM/I Brightness Temperatures and Sea Ice Concentration Grids for the Polar Regions on CD-ROM User's Guide*, NSIDC Distributed Active Archive Center, University of Colorado at Boulder. Digital data available from nsidc@kryos.colorado.edu.

NSIDC: 1997, *Passive Microwave Derived Daily Polar Sea Ice Concentration Time Series*, NSIDC Distributed Active Archive Center, University of Colorado at Boulder. Digital data available from nsidc@kryos.colorado.edu.

Parkinson, C. L.: 1992, 'Interannual Variability of Monthly Southern Ocean Sea-Ice Distribution', *J. Geophys. Res.* **97**, 5349–5363.

Parkinson, C. L.: 1994, 'Spatial Patterns in the Length of the Sea Ice Season in the Southern Ocean, 1979–1986', *J. Geophys. Res.* **99**, 16327–16339.

Parkinson, C. L., Comiso, J. C., Zwally, H. J., Cavalieri, D. J., Gloersen, P., and Campbell, W. J.: 1987, *Arctic Sea Ice, 1973–1976: Satellite Passive-Microwave Observations, (NASA SP-489)*, National Aeronautics and Space Administration, Washington, D.C., 296 pp.

Pittock, A. B.: 1973, 'Global Meridional Interactions in Stratosphere and Troposphere', *Quart. J. R. Met. Soc.* **99**, 424–437.

Rogers, J. C.: 1983, 'Spatial Variability of Antarctic Temperature Anomalies and Their Association with the Southern Hemisphere Atmospheric Circulation', *Ann. Assoc. Amer. Geogr.* **73**, 502–518.

Ross, R. M. and Quetin, L. B.: 1991, 'Ecological Physiology of Larval Euphausiids, *Euphausia superba* (Euphausiacea)', *Memoirs Queensland Museum* **31**, 321–333.

Siegel, V. and Loeb, V.: 1995, 'Recruitment of Antarctic Krill Euphausia Superba and Possible Causes for Its Variability', *Mar. Ecol. Prog. Ser.* **123**, 45–56.

Sissala, J. F., Sabatini, R. R., and Ackerman, H. J.: 1972, 'Nimbus Satellite Data for Polar Ice Survey', *Polar Rec.* **16**, 367–373.

Smith, R. C., Baker, K. S., Fraser, W. R., Hofmann, E. E., Karl, D. M., Klinck, J. M., Quetin, L. B., Prezelin, B. B., Ross, R. M., Trivelpiece, W. Z., and Vernet, M.: 1995, 'The Palmer LTER: A Long-Term Ecological Research Program at Palmer Station, Antarctica', *Oceanography* **8**, 77–86.

Smith, R. C., Stammerjohn, S., and Baker, K. S.: 1996, 'Surface Air Temperature Variations in the Western Antarctic Peninsula Region', in Ross, R. M., Hofmann, E. E., and Quetin, L. B. (eds.), *Foundations for Ecological Research West of the Antarctic Peninsula, AGU Antarctic Research Series*, pp. 105–121.

Stammerjohn, S. and Smith, R. C.: 1996, 'Spatial and Temporal Variability of Western Antarctic Peninsula Sea Ice Coverage', in Ross, R. M., Hofmann, E. E., and Quetin, L. B. (eds.), *Foundations for Ecological Research West of the Antarctic Peninsula, AGU Antarctic Research Series*, pp. 81–104.

Stammerjohn, S., Baker, K. S., and Smith, R. C.: 1997, 'Sea Ice Indexes for Southern Ocean Regional Marine Ecology Studies', *SIO Ref. 97-01*, University of California at San Diego, Scripps Institution of Oceanography, La Jolla, California.

Stark, P.: 1994, 'Climatic Warming in the Central Antarctic Peninsula Area', *Weather* **49**, 215–220.

Stouffer, R. J., Manabe, S., and Bryan, K.: 1989, 'Interhemispheric Asymmetry in Climate Response to a Gradual Increase of Atmospheric $CO_2$', *Nature* **342**, 660–662.

Streten, N. A.: 1973, 'Satellite Observations of the Summer Decay of the Antarctic Sea-Ice', *Arch. Meteorol. Geophys. Bioklimatol. Ser. A* **22**, 119–134.

Stroeve, J., Li, X., and Maslanik, J.: 1997, 'An Intercomparison of DMSP F11- and F13-Derived Sea Ice Products', *Remote Sensing of Environment* (accepted).

Trenberth, K. E.: 1975, 'A Quasi-Biennial Standing Wave in the Southern Hemisphere and Interrelations with Sea Surface Temperature', *Quart. J. R. Met. Soc.* **101**, 55–74.

Trenberth, K. E.: 1979, 'Interannual Variability of the 500 mb Zonal Mean Flow in the Southern Hemisphere', *Monthly Weather Rev.* **107**, 1515–1524.

Trenberth, K. E.: 1980, 'Planetary Waves at 500 mb in the Southern Hemisphere', *Monthly Weather Rev.* **108**, 1378–1389.

Trenberth, K. E.: 1981, 'Interannual Variability of the Southern Hemisphere 500 mb Flow: Regional Characteristics', *Monthly Weather Rev.* **109**, 127–136.

Trenberth, K. E.: 1984, 'The Atmospheric Circulation Affecting the West Antarctic Region in Summer', *Environment of West Antarctica, Potential $CO_2$-Induced Changes: Report of a Workshop*

*Held in Madison, Wisconsin 5–7 July 1983*, National Research Council, National Academic Press, Washington, D.C., pp. 73–87.

van Loon, H. and Jenne, R. L.: 1972, 'The Zonal Harmonic Standing Waves in the Southern Hemisphere', *J. Geophys. Res.* **77**, 992–1003.

van Loon, H., Taljaard, J. J., Jenne, R. L., and Crutcher, H. L.: 1971, 'Climate of the Upper Air: Southern Hemisphere. Volume II, Zonal Geostrophic Winds', *NAVAIR 50-1C-56 and NCAR TN/STR-57*, National Center for Atmospheric Research, Boulder, Colorado.

van Loon, H., Kidson, J. W., and Mullan, A. B.: 1993, 'Decadal Variation of the Annual Cycle in the Australian Dataset', *J. Clim.* **6**, 1227–1231.

Wentz, F.: 1995, 'Deriving Earth Science Products from SSM/I', *Progress Report for Contract NASA-4714, August 1993 through January 1995*, pp. 2–4.

White, W. B. and Peterson, R. G.: 1996, 'An Antarctic Circumpolar Wave in Surface Pressure, Wind, Temperature and Sea-Ice Extent', *Nature* **380**, 699–702.

Zabel, I. H. and Jezek, K. C.: 1994, 'Consistency in Long-Term Observations of Oceans and Ice from Space', *J. Geophys. Res.* **99**, 10109–10121.

Zwally, H. J., Parkinson, C. L., and Comiso, J. C.: 1983a, 'Variability of Antarctic Sea Ice and Changes in Carbon Dioxide', *Science* **220**, 1005–1012.

Zwally, H. J., Comiso, J. C., Parkinson, C. L., Campbell, W. J., Carsey, F. D., and Gloersen, P.: 1983b, *Antarctic Sea Ice, 1973–1976: Satellite Passive-Microwave Observations, (NASA SP-459)*, National Aeronautics and Space Administration, Washington, D.C., 206 pp.

(Received 23 September 1996; in revised form 21 March 1997)